Toxoplasma gondii Chinese 1 Genotype Wh6 Strain Causes Mice Abnormal Cognitive Behavior through Affecting Hippocampal Neurons

Qing Tao
Anhui Medical University
Wen Cui
Anhui Medical University
Lei Liu
Soochow University Medical College
Qingli Luo
Anhui Medical University
Mengmeng Jin
Department of Maternity and Child Health Hospital of Anhui Province
Famin Zhang
Anhui Medical University
Jinjin Zhu
Anhui Medical University
Jian Du
Anhui Medical University
Li Yu
Anhui Medical University
Jilong Shen
Anhui Medical University
Deyong Chu (chudeyong14@yahoo.com)
Anhui Medical University

Research

Keywords: Toxoplasma gondii Chinese 1 genotype Wh6 strain, Cognitive behavior disorder, Apoptosis, Aβ

Posted Date: August 28th, 2020

DOI: https://doi.org/10.21203/rs.3.rs-65523/v1

Abstract

Background

Chronic *Toxoplasma gondii* (*T. gondii*) infection evokes abnormal cognitive behavior of the host. Recent studies suggest that the polarization of microglia to the phenotype of classically activated macrophage (M1) and the deposition of beta-amyloid (Aβ) may be induced in brain of mice chronically infected with *T. gondii*. However, so far, there is no definite explanation for the relationship mechanism underlying the above between microglia polarization, Aβ deposition and *T. gondii*. Our previous investigations indicated that *in vitro T. gondii* type □ strain dense granule protein 15 ($GRA15_{□}$), one of the genotype-associated effectors of *T. gondii* □ strain may induce mouse macrophage to M1. While *T. gondii* type □/□ strain rhoptry protein 16 ($ROP16_{□/□}$) can drive the mouse macrophage to the phenotype of alternatively activated macrophage (M2). Unlike the archetypal strains of types □, □, and □, *T. gondii* Chinese 1 genotype Wh6 strain (TgCtwh6) possesses both $GRA15_{□}$ and $ROP16_{□/□}$ proteins, indicating the unique pathogenesis of *Toxoplasma*-related cognitive behavioral abnormalities.

Methods

In this study, we constructed mice model of cognitive behavioral abnormalities through chronic infection of TgCtwh6 via the oral route, and used mouse hippocampal neuronal cell line (HT22) and mouse microglial cell line (BV2) infected with TgCtwh6 in co-culture system to explore the mechanism with which TgCtwh6 infection induced mouse abnormal cognitive behavior. The immunohistochemistry, immunofluorescence, western blotting, cell culture assays, as well as an array of mouse behavior tests were adopted in the research.

Results

In our research, the infected group showed abnormal cognitive behavior in the water maze and open field experiments in comparison with the control group. Further study showed that the number of synapses and hippocampal neurons decreased and the expression of Aβ increased in brain. *In vitro*, our research indicated that TgCtwh6 infection could not only directly lead to the HT22 apoptosis but also directly induce BV2 activation to M1 possibly through Notch pathway. Activated BV2 secreted pro-inflammatory factors resulting in HT22 apoptosis indirectly in transwell device. Meanwhile, our reseach demonstrated that TgCtwh6 infection caused a notable expression of β-secretase 1 (BACE1)□amyloid precursor protein (APP) and Aβ in HT22 through NF-κB signaling. Furthmore, BV2 activated by TgCtwh6 infection produced pro-inflammatory factors, such as IL-6, TNF-α and iNOS, which promoted HT22 to express APP in co-culture system. In all, our results suggested that TgCtwh6 gave rise to mouse abnormal cognitive behavior due to hippocampal neuronal apoptosis and Aβ deposition driven by indirect and indirect TgCtwh6 infection to hippocampal neuron. In this pathogenic process, microglia activation played an important role in mediating hippocampal neuronal apoptosis and Aβ deposition.

Conclusions

This study demonstrates TgCtwh6 infection can cause mice to develop AD-like symptoms and give rise to hippocampal neuronal apoptosis and Aβ deposition. Besides, microglia activation played an functional role in the pathological development.

Introduction

The neurotropic parasite *Toxoplasma gondii* (*T. gondii*) can invade almost all warm-blooded animals, including human. The chronic infection of *T. gondii* is almost up to one-third of the global population [1, 2]. *T. gondii* can enter various anatomical sites (for example, cerebral cortex, hippocampus, amygdale and so on) of brain to form tissue cysts through the blood-brain barrier and erode neurons, astrocytes, and microglia [3–5]. Increasing evidence indicates that chronic *T. gondii* infection can cause cognitive behavioral abnormalities, such as epilepsy, schizophrenia, and even induce suicide, traffic and industrial accidents[6–8]. Numerous epidemiological statistics suggest that the positive rate of serum Toxoplasma antibodies in Alzheimer's disease (AD) patients was higher than that in the control group[9]. *T. gondii* infection can induce or aggravate human cognitive impairment, memory loss, and learning decline[10]. Obviously, it is necessary and meaningful to study the relationship between *T. gondii* and cognitive behavioral abnormalities.

Cognitive behavioral abnormalities mainly include changes in memory, comprehension, learning, and judgment, and are accompanied by abnormalities in emotions and behaviors[11]. AD is a type of neurodegenerative disease, presenting an abnormal cognitive behavior with a slow progression and worsening over time. The World Heath Organization manifested that it would arrive at 74.7 million and 114 million people living with AD worldwide by the year 2030 and 2050, respectively[12]. Although AD has affected millions of people every day, the etiology and pathogenesis of AD remain elusive. At present, the most common hypotheses about the cause of AD are the amyloid plaque hypothesis and [13–16]. Bacteria, viruses and parasites have also been demonstrated to be involved in AD[17, 18]. *T. gondii* ME49 strain can induce two major hallmarks of AD to produce, beta-amyloid protein (Aβ) and hyperphosphorylated Tau protein[19, 20]. The main pathological features of AD are neuronal cell loss, excessive deposition of Aβ, neurofibrillary and neuroinflammation accompanied with clinical manifestation of abnormal cognitive behaviors. Aβ is derived from amyloid precursor protein (APP) through proteolytic cleavage by β-secretase 1 (BACE1). It has been reported that in neurological diseases, NF-κBp65 can increase Aβ production by up-regulating the activity of the BACE1 promoter [21, 22]. Neuronal loss and synapse density decline were also found in the brain of mice infected with *T. gondii* Pru strain, which could cause cognitive behavioral abnormalities[23]. The inflammation response of microglia is implicated in the development of AD, too [24]. BV2, a mouse microglial cell line, exhibits a classically activated macrophages (M1) status and secretes pro-inflammatory factors such as IL-6, TNF-α, and iNOS after stimulation by LPS, IFN-γ, or parasites [25, 26]. Furthermore, the Notch signaling pathway is closely related to the activation of microglia and the secretion of pro-inflammatory mediators from microglia[27].

The predominant genotype of *T. gondii* prevalent in China is Chinese1 (ToxoDB # 9) found by our research group. The genotype has two representative strains, *T. gondii* Chinese 1 genotype Wh3 strain (TgCtwh3) and *T. gondii* Chinese 1 genotype Wh6 strain (TgCtwh6), both of them have *T. gondii* type □ strain dense granule protein 15 ($GRA15_{□}$) and *T. gondii* type □/□ strain rhoptry protein 16 ($ROP16_{□/□}$) polymorphisms[28]. Some studies ascertained that $GRA15_{□}$ can directly activate NF-κB pathway [9, 29]. Also, our previous research results show that $GRA15_{□}$ can induce mouse macrophages to M1 *in vitro* [30, 31]. As is known, the relative intensity of virulence in some *T. gondii* stains prevalent in the world is compared as following: RH > TgCtwh3 > TgCtwh6 > Pru[32]. But the relationship between TgCtwh6 and cognitive behavior has not been studied so far. So, in this study we will focus on the effect of TgCtwh6 on cognitive behavior in mice and try *in vivo* and *in vitro* to explore the mechanism with which TgCtwh6 cause the changes of mice cognitive behavior at cellular and molecular level.

This study would be conducive for a better understanding of the pathogenesis of cognitive behavioral abnormalities, including AD caused by a special *T. gondii* genotype strain predominantly circulating in China. And also this study would offer an experimental and theoretical basis for the prevention and treatment of the Chinese cognitive behavior disorders in the future.

Materials And Methods

Animals and T. gondii-infected Challenge

C57BL/6, 8 to 12-week-old (Specific Pathogen Free, SPF) male mice were purchased from the Changzhou Cavens Laboratory Animal Company, China (production permit number: Scxk 2016-0010). The mice were housed under controlled conditions (12/12 h light/dark cycle and 22 ± 2 °C temperature) and fed with standard food and pure water. All mice were randomly divided into two groups, twenty four in each: the control group and the infected group. Each mouse in the infection group was infected orally with 30 cysts of TgCtwh6 in 0.3 ml normal saline; meanwhile, the mice of the control group were given orally 0.3 ml normal saline. All mice were implemented cognitive behavioral tests at 90 days and euthanized at 97 days post-infection. The brain tissue was collected for cysts examination under a light microscope at a magnification of 40 × 100. The right brain was collected and fixed in 4% paraformaldehyde for 24 h at room temperature, and then the brain was embedded in paraffin for HE and immunohistochemical examinations. The remaining brain tissues were stored at -80℃ for RNA and protein assays.

Materials

Hematoxylin and eosin (HE) and Nissl staining kit, ThioflavinS, ammoniumpyrrolidinedithiocarbamate (PDTC, a inhibitor of NF-κB pathway), 3, 3'-diaminobenzidine tetrahydrochloride (DAB), penicillin and streptomycin were purchased from Sigma (St. Louis, MO, USA). Dulbecco's modifed Eagle's medium (DMEM) and fetal bovine serum (FBS) were obtained from Wisent (Montreal, QC, Canada). BCA protein assay kit, 2-(4-Amidinophenyl)-6-indolecarbamidine dihydrochloride (DAPI) and SDS polyacrylamide gel

electrophoresis werepurchased from Beyotime (Shanghai, China). RIPA Lysis Buffer and Nitrocellulose membrane were provided by Millipore (Billerica, MA, USA). Anti-NF-κBp65, phospho-NF-κBp65, BACE1, APP, Caspase3, Bax, Bcl-XL, Notch, Hes1 and GAPDH antibodies were purchased from Cell Signaling Technology (Beverly, MA, USA). Anti-Aβ antibody was purchased from Abcam (Cambridge, MA, USA). Anti-Synaptotagmin1, and horseradish peroxide (HRP)-conjugated goat anti-rabbit IgG were purchased from Proteintech (Chicago, IL, USA). Alexa Fluor 488-conjugated anti-rabbit antibody was purchased from Invitrogen (Carlsbad, CA, USA). Prime Script first Strand cDNA Synthesis Kit and SYBR Premix Ex Taq kit was purchased from TaKaRa (TaKaRa Bio, Japan). FITC-labeled anti-mouse CD80, APC-labeled antimouse CD206 and Annexin V-FITC Apoptosis Detection Kit I were obtained from BD Biosciences (New York, BD, USA) for flow cytometry (FCM) analysis. The tachyzoites and cysts of TgCtwh6 were maintained in human foreskin fibroblast line (HFF) and mice, respectively, in our lab. Hippocampal neuronal cell line (HT22) was purchased from Procell (Wuhan, China). HFF and mouse microglial cell line (BV2) were obtained from Chinese Academy of Sciences (Shanghai, China).

Open Field Test

Open Field test (OFT) was fulfilled on the Open Field apparatus (Shanghai Bio will Co., Ltd., Shanghai, China). Briefly, Mobility in an open field was measured under the same time and light condition at 90 days post-TgCtwh6 infection. Each mouse was placed in the center of an open field arena (18 × 18 × 18 inch). The movement of the mouse was recorded by a USB webcam (Logitech HD-1820p) and PC-based video capture software. The recorded video file was further analyzed by video tracking software (Topscan, Clever Systems) to determine the velocity and the total distance traveled by each mouse during the 5-min observation period. The percentage of time spent in the corner and the center of the open field was also recorded. Both the test and the analysis were performed by an observer blinded to the treatment conditions.

Morris Water Maze Test

Morris Water Maze Test (MWMT) was carried out on the Morris Water Maze device (YiShu Information Technology Co. Ltd., Shanghai, China). Cognitive performance was evaluated by the Morris Water Maze test at 90 days post-TgCtwh6 infection. The whole experiment is divided into two parts: the hidden platform trial and the probe trial. Firstly, the hidden platform trial was conducted, and mice (n = 24 per group) were individually released from a randomly selected quadrant to find the hidden platform (2 cm below the water surface) for 60 s and then stay on the platform for 20 s for 5 consecutive days. Each mouse received four learning sessions separated by 30 s intervals each day. For each trial, the mouse was placed in the pool (facing the pool wall) at one of the selected quadrants. Each trial lasted until the mouse found the platform or until a maximum of 60 s. If the mouse failed to find the platform within 60 s, it was guided to the platform by a technician for 15 s. The time spent in reaching the platform was recorded as mice escape latency. The probe trial was further conducted on the sixth day, and the hidden platform was removed. All mice were allowed to swim freely for 60 s. The frequency of an individual mouse passing the platform area and the time mice spent in the target quadrant were recorded as a measure of spatial memory.

HE and Immunohistochemistry (IHC)

In general, brain tissues embedded in paraffin blocks were cut into 4 μm thickness sections to examine the histopathological changes by HE staining. Additionally, in immunohistochemistry assay, brain tissue sections were dewaxed in xylene for three times and rehydrated in gradient concentrations of ethanol. Sections were incubated in sodium citrate solution buffer at 92 °C for 10 min. In order to deactivate endogenous peroxidase, 0.3% H_2O_2 was dropwise added in tissue sections. Following, sections were incubated with Anti-Aβ (1:200) overnight at 4 °C, followed by incubating with HRP-conjugated goat anti-rabbit secondary antibody for 45 min. Then, the sections were color developed with DAB. The total number of Anti-Aβ positive areas in the hippocampus was counted in 5 different fields of view for each section randomly by an observer in a blinded manner via light microscopy. Finally, all HE and immunostained tissue sections were observed under light microscopy at a magnification of 20 × 100 and 40 × 100 and images were captured by an observer in a blinded manner. Quantitative and qualitative changes were analyzed using morphometric software (Image-Pro Plus software, Media Cybernetics, Inc.,Rockville, MD, USA).

Nissl Staining

Nissl staining was performed to observe changes in the number of neurons after TgCtwh6 infection. Brain sections were made as previously described. The frozen sections were stained with 0.1% cresyl violet for 20 min, rinsed with PBS, dehydrated in a graded alcohol series, cleared with xylene, and mounted with neutral gum. Finally, all sections were observed under light microscopy at a magnification of 20 × 100 and 40 × 100 and the total number of Nissl staining positive areas in the section was counted in 5 different fields of view for each section randomly by an observer in a blinded manner via light microscopy.

Thioflavin S plaque Staining

Firstly, thioflavin S was prepared with 50% alcohol with a concentration of 0.3%. Then the sections were incubated with the Thioflavin S at room temperature for 8 min, followed by counterstaining nuclei with DAPI. The sections were placed in PBS and washed 3 times for 5 min each. Finally, they were observed under fluorescence microscope at a magnification of 20 × 100 and 40 × 100 (Leica, Germany) and images were photographed by an observer in a blinded manner. The total number of positive areas stained by Thioflavin S in the section was counted in 5 different fields of view for each section randomly.

Immunofluorescence Staining

TgCtwh6 were harvested from the continuous cell cultures in HFF. HT22 were seeded in a 12-well plate and divided into two groups, the infected and control group. These cells were cultured with DMEM supplemented with 10% FBS, 100 μg/ml streptomycin and 100 U/ml penicillin. After HT22 were cultured 24 h, TgCtwh6 were added into the plate and cocultured with HT22 for another 24 h. Then the HT22 were washed by PBS and fixed in 4% paraformaldehyde. After cell membranes were penetrated by 0.5% Triton

X-100, these cells were incubated with anti-Aβ, NF-κBp65 and BACE1 antibody, respectively, for 16 h. Then, these cells were incubated with Alexa Fluor 488-conjugated anti-rabbit antibody for 1 h at room temperature, followed by counterstaining nuclei with DAPI. These sections were observed under a fluorescence microscope at a magnification of 20 × 100 and 40 × 100 and images were photographed by an observer in a blinded manner. The total number of immunofluorescence staining positive areas in the section was counted in 5 different fields of view for each section randomly.

Western Blotting Analysis

Around 100 mg of hippocampus tissue or the cultured HT22 cells were lysed in the ice-cold RIPA Lysis Buffer supplemented with protease inhibitors, and the total protein concentrations were detected using BCA protein assay kit. The proteins (20 μg) from each sample were added to 10% polyacrylamide gels, then separated and electrophoretically transferred into a nitrocellulose membrane. Non-specific binding in protein-transferred nitrocellulose membranes was blocked with 5% skim milk in PBS-Tween-20 (0.1%) for 2 h at room temperature. The membranes were incubated with primary antibodies to NF-κBp65 (1:1,000), APP (1:1,000), BACE1 (1:1000), Bax (1:1000), Bcl-XL (1:1000), Caspase3 (1:1000), Synaptotagmin1 (1:1000) and GAPDH (1:2,000) at 4 °C overnight, then with HRP-conjugated secondary antibody for 1 h at room temperature. The specific protein signals were captured by ECL kit. The protein bands in images were visualized by Bio-Rad XRS imaging system and the proteins intensity was semi-quantitatively evaluated by image J software.

Quantitative Real-Time PCR (RT-qPCR)

RNA of the hippocampus tissue, BV2 and HT22 cells were extracted using the TRIzol reagent, followed by determining RNA concentration and purity by NanoDrop2000 (Thermo Scientific, Shanghai, China). RNA 1 μg was reversely transcribed to cDNA using Prime Script first Strand cDNA Synthesis Kit. The qRT-PCR was performed to detect the expression of NF-κBp65, BACE1, APP, IL-6, TNF-α, iNOS and TGF-β1 using SYBR Premix Ex Taq kit via Light Cycler 480 (Roche, Switzerland), and the thermal cycling condition was programmed following the manufacturer's protocol. Cycle threshold values were counted through $2^{-\Delta\Delta CT}$ method to analyze the relative genes expression. GAPDH, a housekeeping gene, was used as a control for the relative quantitative evaluation of the transcript abundance of target RNA. All qRT-PCR were conducted in technical triplicates. Sequences of gene-specific primers are listed in Table 1.

Table 1
The primers used for qRT-PCR.

Primers	Forward primer(5'-3')	Reverse primer(5'-3')
APP	TGAATGTGCAGAATGGAAAGTG	AACTAGGCAACGGTAAGGAATC
BACE1	GCAGACATGGAAGACTGTGGCTAC	GGCAGAGTGGCAACATGAAGAGG
IL-6	CCGGAGAGGAGACTTCACAG	CATTTCCACGATTTCCCAGA
TNF-α	ACGGCATGGATCTCAAAGAC	GTGGGTGAGGAGCACGTAGT
iNOS	CACCTTGGAGTTCACCCAGT	ACCACTCGTACTTGGGATGC
TGF-β1	CTGGATACCAACTACTGCTTCAG	TTGGTTGTAGAGGGCAAGGACCT
GAPDH	CAACTTTGGCATTGTGGAAGG	ACACATTGGGGGTAGGAACAC

Cells Culture and Co-culture System

BV2 and HT22 were cultured separately in DMEM medium supplemented with 10% FBS, 2 mM L-glutamine (Gibco, Grand Island, New York, NY, USA), 100 μg/ml streptomycin and 100 U/ml penicillin at 37 °C with 5% CO_2. The transwell device (Corning, Corning, NY, USA) was used to establish a co-culture system. The pore size of the polycarbonate filter membrane in the upper chamber is 0.4 μm, which allowed small and soluble molecules but not cells to pass through. Firstly, BV2 (1×10^6) were seeded into a 12-well plate and cultured for 12 h, and then TgCtwh6 (1×10^6) were added into the same plate and co-cultured for another 24 h followed by evaluating gene expression of IL-6, TNF-α, iNOS and TGF-β1 in BV2 using qRT-PCR, polarization state of BV2 using FCM. Secondly, in the subsequent experiments, HT22 cells were seeded in a 12-well plate and divided into four groups: control group, PDTC group, infection group, and PDTC + infection group. After 12 h, PDTC (10 mmol/L), an inhibitor of NF-κB, was added into each well of PDTC group or PDTC + infection group to pretreat cells for 12 h. Then the cell culture supernatants of the four groups were discarded, and these cells continued to be cultured in replenished DMEM. At the same time, TgCtwh6 (1×10^6) were added into the infection group and PDTC + infection group, respectively. After cultured for another 24 h, HT22 cells in the four groups were collected and the protein expression of *p*-NF-κBp65, NF-κBp65, BACE1, APP were detected by western blotting, and also *p*-NF-κBp65, NF-κBp65, BACE1, Aβ proteins were analyzed by immunofluorescence staining. In the transwell device, BV2 (1×10^6) were cultured in the upper. After 12 h, TgCtwh6 (1×10^6) were added into the upper chamber and co-cultured with BV2 for another 24 h, and then culture supernatants were discarded. Next, the infected BV2 was co-cultured in replenished DMEM for another 24 h with the HT22 seeded in the lower layer of transwell system. HT22 in lower chamber were harvested for apoptosis analysis by western blotting and FCM.

FCM Assay

BV2 with or without TgCtwh6 infection were collected and washed in PBS containing 1% FBS, then adjusted to 1×10^6 cells per 100 μl PBS. The cells were subjected to FITC-labeled anti-mouse CD80 and

APC-labeled anti-mouse CD206 for surface antigens staining. All cells were incubated with these antibodies at 4 °C for 30 min and protected from light, then washed twice in PBS before detected by FCM for polarization state of BV2. Apoptosis of HT22 directly infected with TgCtwh6 or cultured in the lower chamber of the transwell device were assessed using FITC Annexin V apoptosis detection kit with CytoFLEX flowcytometry (Beckman Coulter, USA), and results were shown using CytExpert 2.1 software.

Statistical Analysis

All data were obtained from triplicate values representing three independent experiments with the identical conditions. *T*-test or one-way ANOVA followed by the Bonferroni post hoc test were used for data analysis using SPSS ver. 17 (Chicago, IL, USA). All results were assessed as mean ± SD (n = 4 replicates for each group), two-tailed $P < 0.05$ or $P < 0.01$ or $P < 0.001$ was regarded as statistically significant.

Results

TgCtwh6 infection impaired cognitive and spatial memory

To identify whether the TgCtwh6 infection can lead to damage of cognitive and spatial memory, we infected the mice with TgCtwh6. After 90 days post-infection, compared with the control group, the infected mice usually showed a typical hunchback posture: ruffled piloerection of the fur, stiff limbs, particularly the hind limbs and whitish eyeball (Fig. 1A). Then, the OFT was conducted to determine the mouse ability of motor and exploration. The result showed no significant difference between the two groups at average speed and total distance they traveled, which suggested all of them owned a similar motor ability (Fig. 1B, C); meanwhile, the experiment indicated that the infected mice exhibited a corner preference and a decrease in the social scope signifying that the infected mice were in their inability to explore due to anxiety (Fig. 1D, E).

Then, we carried out the MWMT to evaluate the ability of learning and memory. The result demonstrated that during the first five days in the hidden platform trial, the infected group spent more time in identifying and locating the platform than the control, revealing the mice memory had been impaired by *TgCtwh6* infection (Fig. 1F). However, the swimming speed and total distance had no obvious difference between two groups, indicating again that the motor ability of the two groups was similar (Fig. 1G, H). The infected mice spent less time in the target area and had less number of crossing hidden-platform than the control mice in the probe trial, displaying the infected mice learning and memory retention had been damaged (Fig. 1I, J). Furthermore, there was no visual disability in the two groups. In all, these results confirmed that TgCtwh6 can damage mice cognitive and spatial memory. Cysts in squashed brain tissue were observed under a light microscope and the results exhibited that several TgCtwh6 cysts existed in the infected mice brain; while no cysts appeared in the brain of the control mice (Fig. 1K).

Histopathological changes were drove by the TgCtwh6 in the hippocampus

The hippocampus tissue pathology was evaluated in the following experiments. HE staining of brain tissue showed that in the normal group the hippocampal neurons were uniformly stained with complete structure and clear nuclear membrane boundaries. On the contrary, the hippocampal neurons were disorganized in the arrangement, reduced in the number and size, and stained deeply in nuclei in the infected group (Fig. 2A). The result indicated that TgCtwh6 infection could induce histopathological changes in the mice hippocampus. Compared with the control group, the number of Nissl bodies in the brain tissue sections of the infected group decreased (Fig. 2B, C), which also indicated that TgCtwh6 infection could lead to a drop in the number of hippocampal neurons. To confirm whether the neuron loss is related with apoptosis, we checked the apoptosis-related proteins in mice hippocampal tissue. The result showed that Bax and Caspase3 were enhanced, while Bcl-XL was diminished, implying TgCtwh6 infection could provoke hippocampal nervous cells, probably including neurons apoptosis (Fig. 2D-G). Furthermore, synaptotagmin1, a synapse-specific marker, apparently declined in the brain of infected mice rather than the control (Fig. 2H, I), suggesting that TgCtwh6 infection could contribute to decrease the number and function of nerve synapses.

TgCtwh6 infection induced Aβ immunoreactivity in the hippocampus

The deposition of Aβ in brain tissue is one of the most important pathological features of brain tissue in Alzheimer's patients with cognitive behavioral disorders. In order to verify whether TgCtwh6 infection would cause the deposition of Aβ, firstly, we compared the production of Aβ in two groups by IHC staining and Thioflavin S plaque staining. The results of IHC staining showed that compared with the control group, Aβ protein in the hippocampus of infected mice illustrated significantly higher expression (Fig. 3A, B). Furthermore, Thioflavin S plaque staining, a 'gold-standard' detection for Aβ, manifested that compared with the control group, a large number of bright green plaques stained with thioflavin S in the hippocampus of the TgCtwh6 infected group (Fig. 3C, D), indicating that Aβ protein expression significantly increased in the infected mice brain. Finally, western blotting and qRT-PCR results clarified that the expression levels of BACE1, APP protein and genes in the hippocampus of mice infected with TgCtwh6 significantly were up-regulated compared with those in the control group (Fig. 3E-I). In short, the deposition of Aβ is another pathological basis for cognitive behavior abnormalities.

TgCtwh6 directly infected HT22 inducing apoptosis

As the number of hippocampal neurons decreased after TgCtwh6 infection, we herein investigated the mechanism with which the neuron lost. After TgCtwh6 tachyzoite infected HT22 cells for 24 h *in vitro*, the apoptosis-related proteins of HT22, such as Bax, Bcl-XL and Caspase3 were detected with western blotting. The results showed that the expressions of pro-apoptotic proteins Bax and Caspase3 were significantly increased in the infected group compared to that in the control group, while the expression of anti-apoptotic protein Bcl-XL was markedly reduced in the infected group compared with that in the

control group (Fig. 4A-D). Besides, compared with the control group, the protein level of synaptotagmin1 in HT22 also decreased in the infected group, suggesting that the number and function of neuron reduced because of TgCtwh6 infection (Fig. 4E-F). Taken together, the results indicated that TgCtwh6 could directly induce HT22 apoptosis, which resulted in hippocampal neurons loss and disfunction.

The expression of apoptosis-related proteins in HT22 cells were measured by western blotting (A-D). Besides, synaptotagmin1 protein was detected by western blotting, too (E-F). Data represent mean ± SD from multi-group experiments. *$p < 0.05$, **$p < 0.01$, and ***$p < 0.001$ (n = 3 each group).

TgCtwh6 infection induced BV2 polarization to M1 phenotype possibly via Notch pathway

There are some clear evidences that the inflammatory response of microglial is one of the vital pathogenesis of AD. We herein researched the potential role of the TgCtwh6 in inducing BV2 polarization. In our experiments, BV2 cells polarization status was determined by FCM according to the expression level of CD80 and CD206. The data indicated that the expression level of CD80 was significantly increased, while the expression level of CD206 remarkably decreased in BV2 infected with TgCtwh6 (Fig. 5A-C). As we all know, CD80 is a marker of M1 and CD206 is a marker of M2. So the results manifested that TgCtwh6 infection can cause BV2 to shift towards M1. Subsequently, we analyze the expression of Notch and Hes1, two key signaling proteins in the Notch pathway in BV2, to explore the possible mechanism with which BV2 was polarized. The results showed that the Notch and Hes1 protein expressions in infected BV2 significantly increased compared with the uninfected BV2 (Fig. 5D-F). The experiments revealed that TgCtwh6 infection might induce the polarization of BV2 towards M1 through Notch signaling.

TgCtwh6 infected BV2 causing pro-inflammatory factors secretion which led to HT22 apoptosis

As TgCtwh6 infection can result in BV2 polarization to M1, we further explored whether polarized BV2 would affect HT22 apoptosis. Firstly, we detected gene expressions of IL-6, TNF-α, iNOS, and TGF-β1 in BV2 infected or uninfected with TgCtwh6 using qRT-PCR. The results showed that the gene expressions of pro-inflammatory factor IL-6, TNF-α and iNOS were noticeably increased, while the gene expression of anti-inflammatory factor TGF-β1 gene was notably decreased in BV2 infected with TgCtwh6 (Fig. 6A-D). Next, HT22 and BV2 that had been infected or uninfected with TgCtwh6 for 24 h, were co-cultured in replenished DMEM for another 24 h in transwell system. Then, HT22 were collected from the lower layer and apoptosis status was detected using FCM. The result showed that compared with the control group, the apoptosis rate of HT22 was significantly increased in early and late stages (Fig. 6E-G), indicating that pro-inflammatory factors secreted from polarized BV2 promoted HT22 apoptosis. Meanwhile, the protein expression of Bax and Caspase3 increased, Bcl-XL decreased in HT22 in the lower layer of transwell device compared with the control group (Fig. 6H-K). In summary, BV2 infected by TgCtwh6 could polarize into M1 and produce a large number of pro-inflammatory factors, which caused the HT22 apoptosis. This

strongly suggested that TgCtwh6 may not only directly, but also indirectly induced hippocampal neurons apoptosis through infecting micrglia which then secreted some pro-inflammatory factor in brain.

TgCtwh6 directly infected HT22 upregulating BACE1, APP, and Aβ protein expression

To further ascertain whether TgCtwh6 infection can directly cause Aβ production in HT22, we detected BACE1, APP and Aβ protein and gene expression in TgCtwh6-infected HT22 by western blotting, qRT-PCR and immunofluorescence staining, respectively. The results revealed that BACE1, APP protein and gene expression levels were significantly higher than those in the control group using western blotting and qRT-PCR (Figs. 7A-E). Also, BACE1 and Aβ protein expressions were up-regulated in TgCtwh6-infected HT22 using immunofluorescence staining (Fig. 7F-G). These data strongly suggested that TgCtwh6 infection could directly lead to the production of Aβ in HT22.

TgCtwh6 infected BV2 resulting in the generation of Aβ in HT22

In order to clarify whether TgCtwh6 infection could indirect induce Aβ production in HT22, we collected HT22 from the lower layer in the co-culture system and analyzed the expression of APP using western blotting. The results suggested that the expression of APP significantly increase (Fig. 8A, B) in HT22 stimulated by inflammatory factors secreted from infected BV2. The result suggested that microglia polarized into M1 after TgCtwh6 infection could induce hippocampal neurons to produce APP by secreting inflammatory factor, that is, Aβ deposition in hippocampal regions may account for the indirect effects of TgCtwh6 infection.

TgCtwh6 directly infected HT22 inducing Aβ production via NF-κB signaling

To explore the mechanism by which TgCtwh6 infection induce Aβ immunoreactivity, and APP and BACE1 production in hippocampal neuron, we estimated the effect of NF-κB signaling on production of Aβ in infected HT22. We collected HT22 infected by TgCtwh6 for 24 h and investigated NF-κBp65, *p*-NF-κBp65, APP and BACE1 expression in the HT22 by western blotting. We found that TgCtwh6 infection not only increased APP and BACE1 but also increased NF-κBp65 and *p*-NF-κBp65 expressions in HT22, compared with those in the control, and these protein expressions could be significantly reduced after HT22 were pretreated with PDTC (Fig. 9A-E). Subsequently, the data of immunofluorescence staining displayed that NF-κBp65, BACE1 and Aβ were highly expressed in the cytoplasm of infected HT22; meanwhile *p*-NF-κBp65 expression was enhanced in the nucleus of infected HT22. Especially, all these protein expressions could be obviously prohibited by PDTC (Fig. 9F-M). Both western blotting and immunofluorescence staining analysis showed TgCtwh6 infection would activate NF-κB signaling and promoted Aβ generation.

Discussion

Chronic infection of *T. gondii* has been reported to cause cognitive behavioral abnormalities and is considered a potential cause of many mental illnesses such as AD. A large number of epidemiological statistics show that the seroprevalence of Toxoplasma antibodies in AD patients is significantly higher than that in the control group[33, 34]. This suggests a possible link between *T. gondii* infection and AD. However, there are some data showing the opposite trend[35]. This may be due to the different experimental models and toxoplasma strains used in different experiments. At present, although it is known that there is a relationship between *T. gondii* infection and cognitive behavioral abnormality, the research on the relationship between *T. gondii* Chinese 1 genotype (ToxoDB # 9) and cognitive behavioral abnormality is not enough.

In our studies, we used TgCtwh6, one of representative strains of ToxoDB # 9 to infect mice constructing model of cognitive behavioral abnormalities. Our results indicated that the mice suffered from TgCtwh6 infection showed abnormal appearance and posture compared with the control mice. Furthermore, the OFT displayed that the infected mice appeared obvious corner preference which is related to increased anxiety. It has been reported that the anxiety-like behavior is also common in AD patients[34, 36]; meanwhile, the data from the MWMT revealed that TgCtwh6 infection damaged the mice memory retention and spatial learning. However, the infected mice have normal mobility, suggesting that *T. gondii* infection hardly affects motor function in mice [37, 38]. After dissecting the brain of mice, cysts were found in the infected group, suggesting that the mice were infected successfully with TgCtwh6 which had reached the mice brain tissue. These results verified that TgCtwh6 infection can result in cognitive behavioral impairment in C57BL/6 mice. So in the following experiments, we tried to investigate the mechanism with which TgCtwh6 infection triggers cognitive behavioral abnormalities.

Our histopathological research *in vivo* showed that the hippocampus neurons reduced in number, disordered in the arrangement and deeply stained in the nucleus in the infected mice, which suggested that the changes in morphology and decrease in number of hippocampal neurons might be related to cognitive behavioral abnormalities. It has been reported that Toxoplasma infection can cause neuron loss in mice [39]. As we all know neuron loss, Aβ deposition and neuroinflammation are the vital histopathological features of AD disease[40]; moreover, theneuron apoptosis is the significant cause of neuron loss[41], so we further confirmed whether TgCtwh6 infection can lead to neuronal apoptosis and Aβ deposition in vivo and in vitro.

Our study *in vivo* showed that Bax, Caspase3 expression increased and Bcl-XL expression decreased in infected mice hippocampus tissue, indicating TgCtwh6 infection could cause hippocampal nervous cells (probably including neurons) apoptosis. In addition, the expressions of BACE1, APP and Aβ in mice hippocampus tissue were significantly higher in the infected group than that in the control group, which suggested that Aβ deposition and neuronal apoptosis were implicated in cognitive behavioral abnormalities in mice infected with TgCtwh6. A large number of data have validated that BACE1 is the main (but not the only) secretion enzyme *in vivo*, and Aβ is derived from the sequential cleavage of APP

by BACE1. Aβ has a strong neurotoxic effect after abnormal processing and accumulation in the cellular matrix, and it plays an important role in the progression of AD[42]. Studies have shown that the addition of Aβ to animal and cell models can impede neurotransmission and cause cognitive impairment [43, 44].

In order to verify the mechanism with which TgCtwh6 induce neuron apoptosis and Aβ deposition in neuron, we carried out the separated or co-culture experiments in transwell device with HT22 and BV2 *in vitro*. The results manifested that HT22 apoptosis was initiated and Aβ expression was increased in HT22 when the HT22 was infected with TgCtwh6; moreover, BV2 was activated to M1 with increased expression of IL-6, TNF-α and iNOS when the BV2 was infected with TgCtwh6. Interestingly, the activated BV2 can induce HT22 apoptosis and APP production. Further study confirmed that Aβ expression was increased via NF-κB pathway in HT22 infected with TgCtwh6. In our study, when HT22 was infected with TgCtwh6, the *p*-NF-κBp65 and NF-κBp65 expression were up-regualated in cytoplasm, and then *p*-NF-κBp65 was transferred into nucleus, promoting BACE1, APP and Aβ expression. Now, more and more studies have affirmed that NF-κB signaling is closely associated with Aβ generation in neurological diseases[45, 46]. NF-κBp65 interacts with NF-κB binding elements to regulate BACE1 at the level of transcription and the BACE1 promoter contains specific NF-κB binding elements. The expression of BACE1 and the production of Aβ are induced via the NF-κB pathway[47].

Additionally, many studies have shown that apoptosis is induced via the NF-κB signaling, too. Mathilde et al. reported apoptosis was elicited through NF-κB pathway in cystic fibrosis cells[48]. Shao et al. also showed miR-146a-5p promoted IL-1β-induced chondrocyte apoptosis via the TRAF6-mediated NF-kB pathway[49]. On the contrary, Robert E et al. have demonstrated NF-κB activation after *T. gondii* RH strain infection is involved in the increase of anti-apoptotic gene expression, which plays a pivotal role in the *T. gondii*-mediated blockade of apoptosis[50]. The difference between the two results may be due to the different *T. gondii* genetype and cell strain used in the experiments. Because *T. gondii* type Ⅰ strain dense granule protein 15 (GRA15$_{Ⅰ}$), one of the genotype-associated effectors of *T. gondii* Ⅰ strain, could activate the NF-kB signaling[51], we speculate that GRA15$_{Ⅰ}$ derived from TgCtwh6 might induce HT22 apoptosis and Aβ production through NF-kB signaling. We will explore this hypothesis in our future work. In addition, our previous results show that the GRA15$_{Ⅰ}$ protein derived from *T. gondii* (Pru stain) can effectively promote the polarization of macrophages to M1[52]. Some other studies demonstrated that GRA15$_{Ⅰ}$ can activate the NF-κB pathway of macrophages, thereby inducing the expression of pro-inflammatory M1-type related genes and transferring macrophages to M1. Besides, ROP16$_{Ⅰ/Ⅲ}$ of *T. gondii* type Ⅰ/Ⅲ can directly phosphorylate the STAT6 pathway of macrophages and polarize macrophages to M2[25, 26, 53]. So, further research is required to clarify whether GRA15$_{Ⅰ}$ derived from TgCtwh6 could induce microglia to polarize into M1 via NF-κB signaling.

Neuroinflammation has been considered as a possible pathological mechanism for cognitive behavioral disorders. Microglia, one of inherent immnune cells, is key mediator of the neuroinflammatory response in brain. Inflammatory response of microglia is an important factor in cognitive abnormalities. In our study, we found that microglia can be activated into M1 by TgCtwh6 infection, and can secret some pro-

inflammatory factors which probably induce HT22 apoposis and APP production in HT22. Especially, we found that TgCtwh6 infection activated microglia perhaps via Notch signaling. Some researchers reported that microglia can be activated by infection (eg., parasites), trauma, and other factors, producing a variety of immune effector molecules that not only mediate chronic inflammation and apoptosis, but also lead to degenerative diseases of the nervous system [54]. The pro-inflammatory cytokines, such as IFN-γ, IL-1β, and TNF-α can attenuate microglia's phagocytic activity, and transform microglia into M1 types[55]. Moreover, some studies have identified that BV2 was activated into M1 through Notch pathway [56]. Notch signaling is involved in regulating microglia activation after hypoxia partly through the cross talk between TLR4/MyD88/TRAF6/NF-κB pathways in brain damage[57]. Cao et al. evidenced when LPS stimulated BV2 cells, both Notch and NF-κB/p65 proteins expression increased significantly, and the expression of Hes-1, TNF-α and IL-1β increased successively. Moreover, they considered Notch signaling can trans-activate NF-NF-κB/p65 by amplifying NF-κB/p65-dependent pro-inflammatory functions in activated BV2 cells[58]. What effector molecule derived from TgCtwh6 can activate Notch signaling, and how the Notch signaling lead to NF-κB activation which promote microglia polarization, Aβ generation and neuron apoptosis are very important and interesting topics we will focus on in the future.

Aβ is neurotoxic, which can mediate neuronal apoptosis [26, 59]. Studies have shown that the presence of endogenous Aβ stimulation in the environment can continuously activate the M1 pro-inflammatory response and eventually lead to irreversible neuron loss[55]. Wu et al. further demonstrated that the pro-inflammatory factors from microglia stimulated by Aβ cause extensive death of apoptotic neurons [26]. So, we supposed that HT22 apoptosis is partly induced by excess Aβ secreted from HT22. Furthermore, Aβ may be used as immune micro-endogenous stimuli in the tissue micro-environment to constantly activate microglia to maintain the M1 pro-inflammatory response.

Conclusion

Our study in vivo showed that TgCtwh6 infection caused mice to develop AD-like symptoms. TgCtwh6 induced hippocmapal neurons apoptosis and Aβ deposition that was probably implicated in NF-κB pathway in mice hippocampal neuron. Our experiment in vitro indicated that TgCtwh6 drive BV2 to polarize into M1 possibly via Notch signaling. The polarized BV2 secreted pro-inflammatory factors which led to neuron apoptosis and the increase of APP (Fig. 10). Our results suggested that TgCtwh6 gave rise to mouse abnormal cognitive behavior due to hippocampal neuronal apoptosis and Aβ deposition driven by indirect and indirect TgCtwh6 infection to hippocampal neuron. In this pathogenic process, microglia activation played an important role in mediating hippocampal neuronal apoptosis and Aβ deposition.

This study would provide an explanation for the pathogenesis of abnormal cognitive behavior caused by TgCtwh6 prevalent in China and offer an experimental and theoretical basis for the prevention and treatment of the chronic cognitive behavior disorder in the future.

List Of Abbreviations

AD

Alzheimer's disease

APP

Amyloid precursor protein

Aβ

Beta-amyloid

BACE1

β-secretase 1

BV2

Mouse microglial cell line

DAB

3, 3'-diaminobenzidine tetrahydrochloride

DAPI

2-(4-Amidinophenyl)-6-indolecarbamidine dihydrochloride

DMEM

Dulbecco’s modifed Eagle’s medium

FBS

Fetal bovine serum

FCM

Flow cytometry

GRA15Ⅱ

T. gondii type Ⅱ strain Gense granule protein 15

HE

Hematoxylin and eosin

HFF

Human foreskin fibroblast line

HT22

Mouse hippocampal neuronal cell line

IHC

Immunohistochemistry

MWMT

Morris Water Maze Test

M1

Classically activated macrophage

M2

Alternatively activated macrophage

OFT

Open Field test

PDTC

Ammoniumpyrrolidinedithiocarbamate

ROP16Ⅰ/Ⅲ

T. gondii type Ⅰ/Ⅲ strain rhoptry protein 16

RT-qPCR

Quantitative Real-Time PCR

SPF

Specific Pathogen Free

TgCtwh3

T. gondii Chinese 1 genotype Wh3 strain

TgCtwh6

T. gondii Chinese 1 genotype Wh6 strain

T.gondii

Toxoplasma gondii

Declarations

Acknowledgements

We thank the assistant by of the Center for Scientific Research of Anhui Medical University.

Funding

This work was supported by the Provincial University Natural Science Research Key Project of Anhui (No. kJ2019A0222), the National Science Foundation of China (No. 81471983), the National Basic Research Program of China (No. 2010CB530001), and the Natural Science Foundation of China (NSFC funding NO. 81572801).

Availability of data and materials

The datasets used and/or analyzed during the current study are available from the corresponding author on reasonable request.

Author's contributions

Deyong Chu and Jilong Shen designed the experiments; Qing Tao, Wen Cui, Jinjin Zhu and Famin Zhang conducted the experiments; Qing Tao, Lei Liu, Qingli Luo and Mengmeng Jin performed the analysis; Qing Tao, Wen Cui, and Lei Liu wrote this manuscript. Deyong Chu, Jilong Shen, Jian Du, and Li Yu editing the manuscript.

All authors read and approved the final manuscript.

Ethics approval

All animal work were conducted in strict accordance with the Chinese National Institute of Health Guide for the Care and Use of Laboratory Animals and obtained the permission of the Institutional Review Board of the Institute of Biomedicine at Anhui Medical University (permit number: AMU26093628).

Consent for publication

Not applicable.

Competing interests

The authors declare that they have no competing interests.

References

1. Innes, E., *A brief history and overview of Toxoplasma gondii.* Zoonoses and public health, 2010. **57**(1): p. 1-7.
2. Dubey, J.P., *Toxoplasmosis of animals and humans*. 2016: CRC press.
3. Parlog, A., D. Schlüter, and I.R. Dunay, *Toxoplasma gondii-induced neuronal alterations.* Parasite immunology, 2015. **37**(3): p. 159-170.
4. Wohlfert, E.A., I.J. Blader, and E.H. Wilson, *Brains and brawn: toxoplasma infections of the central nervous system and skeletal muscle.* Trends in parasitology, 2017. **33**(7): p. 519-531.
5. Ingram, W.M., et al., *Mice infected with low-virulence strains of Toxoplasma gondii lose their innate aversion to cat urine, even after extensive parasite clearance.* PloS one, 2013. **8**(9): p. e75246.
6. Flegr, J., *How and why Toxoplasma makes us crazy.* Trends in parasitology, 2013. **29**(4): p. 156-163.
7. Wang, T., et al., *A potential association between Toxoplasma gondii infection and schizophrenia in mouse models.* Experimental parasitology, 2013. **135**(3): p. 497-502.
8. Ngoungou, E.B., et al., *Toxoplasmosis and epilepsy—systematic review and meta analysis.* PLoS Negl Trop Dis, 2015. **9**(2): p. e0003525.
9. Kusbeci, O.Y., et al., *Could Toxoplasma gondii have any role in Alzheimer disease?* Alzheimer Disease & Associated Disorders, 2011. **25**(1): p. 1-3.
10. Gajewski, P.D., et al., *Toxoplasma gondii impairs memory in infected seniors.* Brain, behavior, and immunity, 2014. **36**: p. 193-199.
11. Sue, D., et al., *Understanding abnormal behavior*. 2015: Cengage Learning.
12. Bhushan, I., et al., *Alzheimer's disease: Causes & treatment–A review.* Ann Biotechnol, 2018. **1**(1): p. 1002.
13. Roberts, G., *Neurofibrillary tangles in Alzheimer's disease.* Biomedicine & Pharmacotherapy, 1990. **44**(1): p. 61-62.
14. Hardy, J.A. and G.A. Higgins, *Alzheimer's disease: the amyloid cascade hypothesis.* Science, 1992. **256**(5054): p. 184-186.
15. Haass, C. and D.J. Selkoe, *Cellular processing of β-amyloid precursor protein and the genesis of amyloid β-peptide.* Cell, 1993. **75**(6): p. 1039-1042.
16. Selkoe, D.J., *Alzheimer's Disease–Genotypes, Phenotype, and Treatments.* Science, 1997. **275**(5300): p. 630-631.
17. Zhou, L., M. Miranda-Saksena, and N.K. Saksena, *Viruses and neurodegeneration.* Virology journal, 2013. **10**(1): p. 172.

18. Mattson, M.P., *Infectious agents and age-related neurodegenerative disorders.* Ageing research reviews, 2004. **3**(1): p. 105-120.
19. Tao, Q., et al., *Toxoplasma gondii Chinese I genotype Wh6 strain infection induces tau phosphorylation via activating GSK3β and causes hippocampal neuron apoptosis.* Acta Tropica, 2020: p. 105560.
20. Torres, L., et al., *Toxoplasma gondii alters NMDAR signaling and induces signs of Alzheimer's disease in wild-type, C57BL/6 mice.* Journal of neuroinflammation, 2018. **15**(1): p. 57.
21. Cai, H., et al., *BACE1 is the major β-secretase for generation of Aβ peptides by neurons.* Nature neuroscience, 2001. **4**(3): p. 233-234.
22. Guglielmotto, M., et al., *Aβ1-42-mediated down-regulation of Uch-L1 is dependent on NF-κB activation and impaired BACE1 lysosomal degradation.* Aging cell, 2012. **11**(5): p. 834-844.
23. Wang, T., et al., *From inflammatory reactions to neurotransmitter changes: implications for understanding the neurobehavioral changes in mice chronically infected with Toxoplasma gondii.* Behavioural Brain Research, 2019. **359**: p. 737-748.
24. Akiyama, H., et al., *Inflammation and Alzheimer's disease.* Neurobiology of aging, 2000. **21**(3): p. 383-421.
25. Jensen, K.D., et al., *Toxoplasma polymorphic effectors determine macrophage polarization and intestinal inflammation.* Cell host & microbe, 2011. **9**(6): p. 472-483.
26. Rosowski, E.E., et al., *Strain-specific activation of the NF-κB pathway by GRA15, a novel Toxoplasma gondii dense granule protein.* Journal of Experimental Medicine, 2011. **208**(1): p. 195-212.
27. Li, Y., et al., *Macrophages polarized by expression of toxoGRA15II inhibit growth of hepatic carcinoma.* Frontiers in immunology, 2017. **8**: p. 137.
28. Hunter, C.A. and L.D. Sibley, *Modulation of innate immunity by Toxoplasma gondii virulence effectors.* Nature Reviews Microbiology, 2012. **10**(11): p. 766-778.
29. Shen, J. and L. Wang, *Genotypes and main effectors of Toxoplasma gondii and their pathogenic mechanisms.* Zhongguo ji sheng chong xue yu ji sheng chong bing za zhi= Chinese journal of parasitology & parasitic diseases, 2015. **33**(6): p. 429-435.
30. Bayani, M., et al., *Toxoplasma gondii infection and risk of Parkinson and Alzheimer diseases: A systematic review and meta-analysis on observational studies.* Acta tropica, 2019.
31. Berenreiterová, M., et al., *The distribution of Toxoplasma gondii cysts in the brain of a mouse with latent toxoplasmosis: implications for the behavioral manipulation hypothesis.* PloS one, 2011. **6**(12).
32. Mahmoudvand, H., et al., *Toxoplasma gondii infection potentiates cognitive impairments of Alzheimer's disease in the BALB/c mice.* Journal of Parasitology, 2016. **102**(6): p. 629-635.
33. Robert-Gangneux, F. and M.-L. Dardé, *Epidemiology of and diagnostic strategies for toxoplasmosis.* Clinical microbiology reviews, 2012. **25**(2): p. 264-296.

34. Seibenhener, M.L. and M.C. Wooten, *Use of the open field maze to measure locomotor and anxiety-like behavior in mice.* JoVE (Journal of Visualized Experiments), 2015(96): p. e52434.
35. Parihar, M. and T. Hemnani, *Alzheimer's disease pathogenesis and therapeutic interventions.* Journal of Clinical Neuroscience, 2004. **11**(5): p. 456-467.
36. Kar, N., *Behavioral and psychological symptoms of dementia and their management.* Indian journal of psychiatry, 2009. **51**(Suppl1): p. S77.
37. Whitehouse, P.J., et al., *Alzheimer's disease and senile dementia: loss of neurons in the basal forebrain.* Science, 1982. **215**(4537): p. 1237-1239.
38. Janus, C., et al., *Aβ peptide immunization reduces behavioural impairment and plaques in a model of Alzheimer's disease.* Nature, 2000. **408**(6815): p. 979-982.
39. Händel, U., et al., *Neuronal gp130 expression is crucial to prevent neuronal loss, hyperinflammation, and lethal course of murine Toxoplasma encephalitis.* The American journal of pathology, 2012. **181**(1): p. 163-173.
40. Lue, L.-F., et al., *Inflammation, Aβ deposition, and neurofibrillary tangle formation as correlates of Alzheimer's disease neurodegeneration.* Journal of neuropathology & experimental neurology, 1996. **55**(10): p. 1083-1088.
41. Macaya, A., *Apoptosis in the nervous system.* Revista de neurologia, 1996. **24**(135): p. 1356.
42. Shi, Z., et al., *BAG-1M co-activates BACE1 transcription through NF-κB and accelerates Aβ production and memory deficit in Alzheimer's disease mouse model.* Biochimica et Biophysica Acta (BBA)-Molecular Basis of Disease, 2017. **1863**(9): p. 2398-2407.
43. Zhang, Y., et al., *Microglial activation and inflammatory cytokine expression in the brain of chronic Toxoplasma gondii-infected mice.* Zhongguo ji sheng chong xue yu ji sheng chong bing za zhi= Chinese journal of parasitology & parasitic diseases, 2013. **31**(3): p. 176-9, 184.
44. Hickman, S.E., E.K. Allison, and J. El Khoury, *Microglial dysfunction and defective β-amyloid clearance pathways in aging Alzheimer's disease mice.* Journal of Neuroscience, 2008. **28**(33): p. 8354-8360.
45. Mattson, M.P. and W.A. Pedersen, *Effects of amyloid precursor protein derivatives andoxidative stress on basal forebrain cholinergic systems inALZHEIMERS disease.* International journal of developmental neuroscience, 1998. **16**(7-8): p. 737-753.
46. Tomita, S., et al., *PDZ domain-dependent suppression of NF-κB/p65-induced Aβ42 production by a neuron-specific X11-like protein.* Journal of Biological Chemistry, 2000. **275**(17): p. 13056-13060.
47. Tang, Y. and W. Le, *Differential roles of M1 and M2 microglia in neurodegenerative diseases.* Molecular neurobiology, 2016. **53**(2): p. 1181-1194.
48. Rottner, M., et al., *Exaggerated apoptosis and nf-kb activation in pancreatic and tracheal cystic fibrosis cells.* The FASEB Journal, 2007. **21**(11): p. 2939-2948.
49. Shao, J., et al., *MiR-146a-5p promotes IL-1β-induced chondrocyte apoptosis through the TRAF6-mediated NF-kB pathway.* Inflammation Research, 2020: p. 1-12.

50. Molestina, R.E., et al., *Activation of NF-κB by Toxoplasma gondii correlates with increased expression of antiapoptotic genes and localization of phosphorylated IκB to the parasitophorous vacuole membrane.* Journal of cell science, 2003. **116**(21): p. 4359-4371.
51. Cai, Y., et al., *ToxoGRA15II promote macrophages polarization against Hepatic carcinoma by targeting TRAF6.* 2019.
52. Liu, L., et al., *Effective amelioration of liver fibrosis through lentiviral vector carrying Toxoplasma gondii gra15II in murine model.* Frontiers in immunology, 2018. **9**: p. 1572.
53. Butcher, B.A., et al., *Toxoplasma gondii rhoptry kinase ROP16 activates STAT3 and STAT6 resulting in cytokine inhibition and arginase-1-dependent growth control.* PLoS Pathog, 2011. **7**(9): p. e1002236.
54. Pereira, C., et al., *Cell degeneration induced by amyloid-β peptides.* Journal of Molecular Neuroscience, 2004. **23**(1-2): p. 97-104.
55. Wu, Q., et al., *Beta-amyloid activated microglia induce cell cycling and cell death in cultured cortical neurons.* Neurobiology of aging, 2000. **21**(6): p. 797-806.
56. Xie, Y., et al., *Toxoplasma gondii GRA15 II effector-induced M1 cells ameliorate liver fibrosis in mice infected with Schistosomiasis japonica.* Cellular & molecular immunology, 2018. **15**(2): p. 120-134.
57. Yao, L., et al., *Notch-1 signaling regulates microglia activation via NF-κB pathway after hypoxic exposure in vivo and in vitro.* PloS one, 2013. **8**(11): p. e78439.
58. Cao, Q., et al., *Nuclear factor-κB/p65 responds to changes in the Notch signaling pathway in murine BV-2 cells and in amoeboid microglia in postnatal rats treated with the γ-secretase complex blocker DAPT.* Journal of neuroscience research, 2010. **88**(12): p. 2701-2714.
59. Alvarez, C., et al., *Striking divergence in Toxoplasma ROP16 nucleotide sequences from human and meat samples.* The Journal of infectious diseases, 2015. **211**(12): p. 2006-2013.

Figures

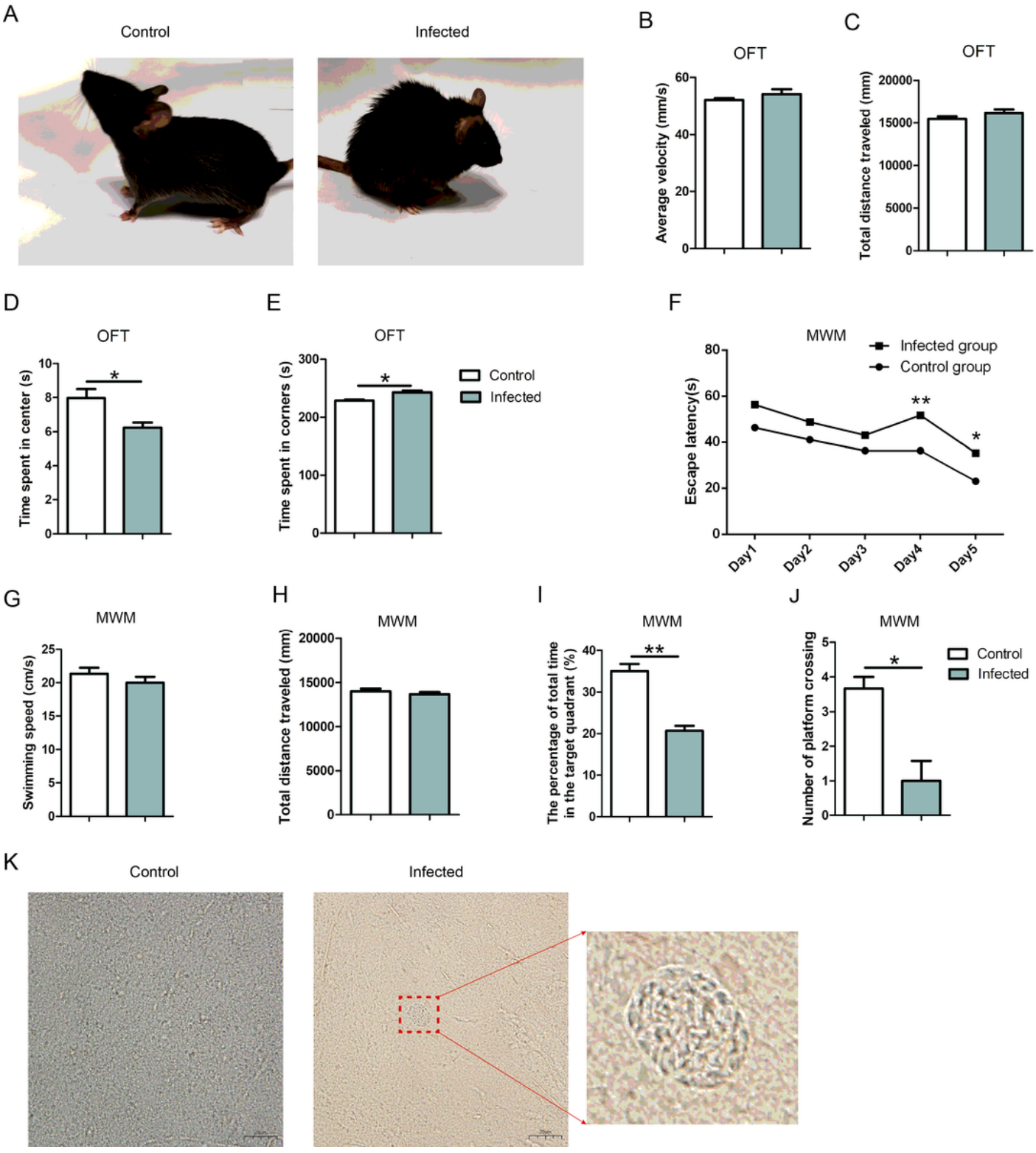

Figure 1

The Effects of TgCtwh6 infection on mice cognitive behavior. TgCtwh6 infection caused mice appearance and posture changes (A). The exploration ability and anxiety-like behavior were evaluated with OFT (B-E); The abilities in learning and memory retention were determined with MWMT (F-J). The brain cysts of mice were assessed by tissue squash method with microscopic examination at a magnification of

40×100 (Scale bars, 20 μm) (K). Data represent mean ± SD from multi-group experiments. *p < 0. 05, **p < 0.01, and ***p < 0.001 (n = 3 each group).

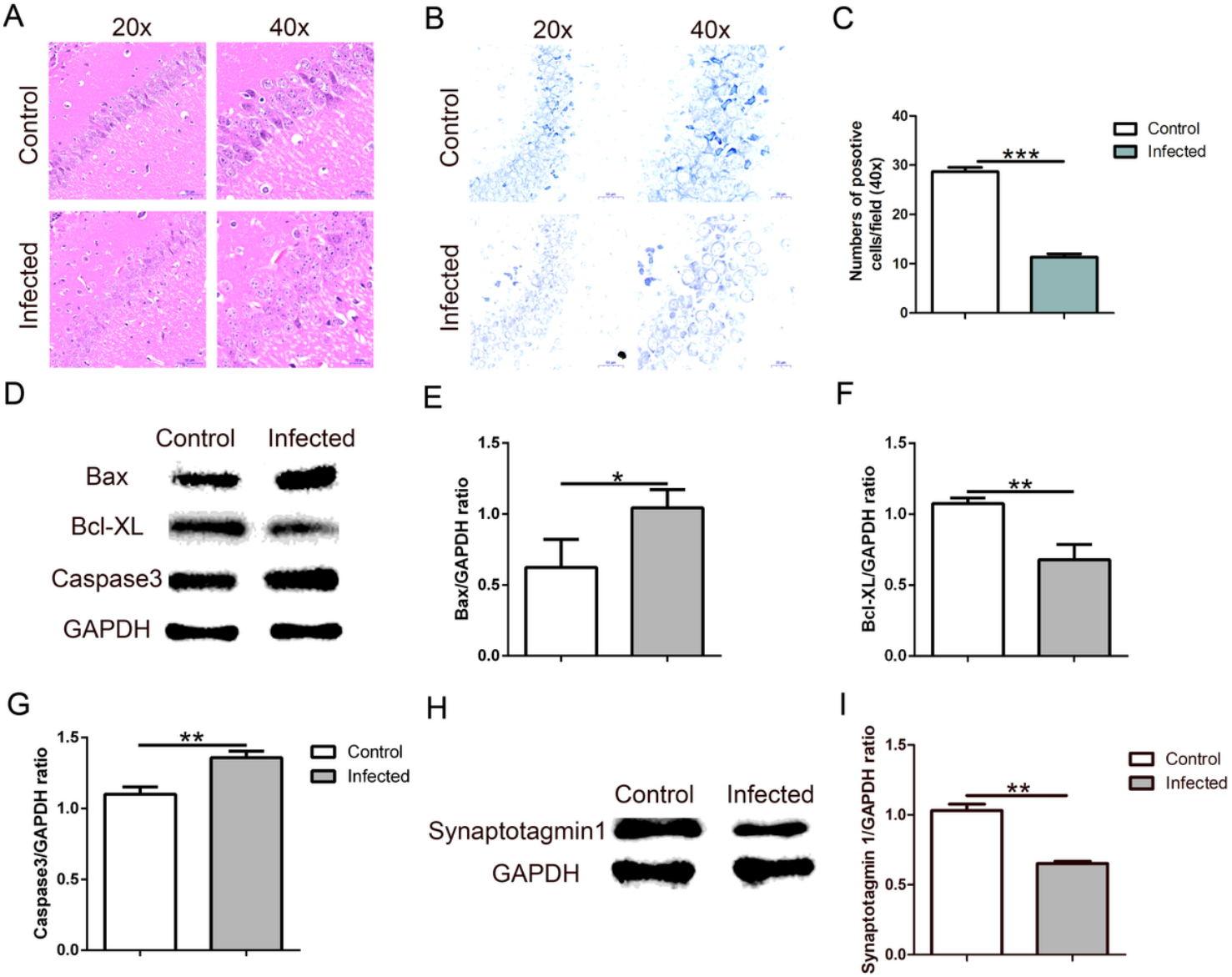

Figure 2

TgCtwh6 infection led to mice hippocampus neuron morpholgical changes and number decrease. The brain tissue section was stained with HE and observed under a light microscope (Scale bars, 20μm) (A). Besides, the brain tissue section was stained with Nissl dye, and the positive area was evaluated with semi-quantitative analysis (Scale bars, 50μm and 20μm, respectively) (B, C). The apoptosis-related proteins were assessed by western blotting and analyzed semi-quantitatively (Figure D-G). Synaptotagmin1 protein was detected by western blotting and analyzed using semi-quantitative method (Figure H, I). Data represent mean ± SD from multi-group experiments. *p < 0.05, **p < 0.01, and ***p < 0.001 (n = 3 each group).

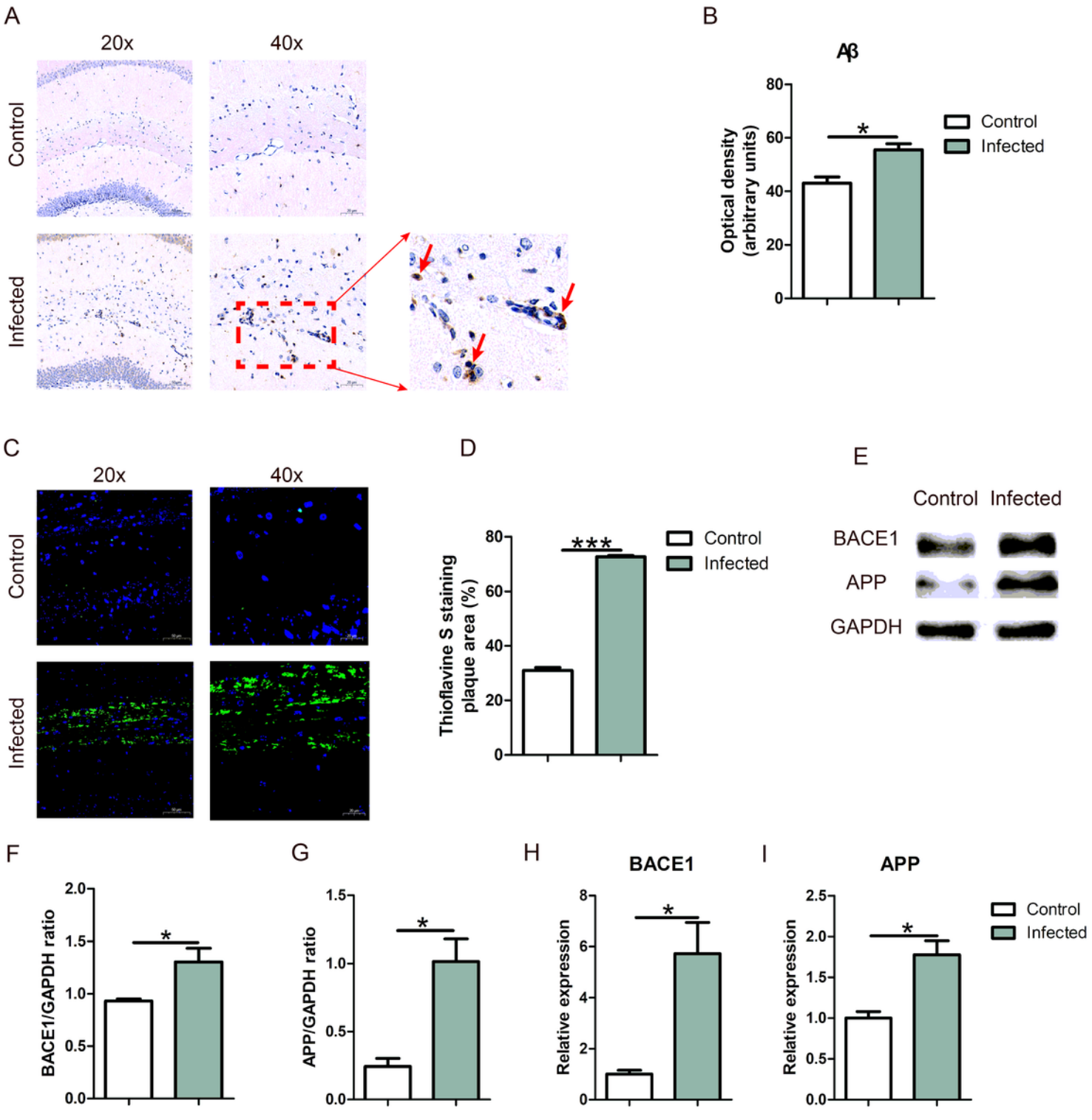

Figure 3

TgCtwh6 infection led to APP, BACE1 and Aβ production in mice hippocampus. Aβ protein level in the mice hippocampal zone was evaluated by IHC and analyzed with semi-quantitative method. The yellow positive cells in mice hippocampus tissue were observed under a light microscopy (Scale bars, 50μm and 20μm, respectively) (A, B). Aβ plaque in brain tissue was detected by Thioflavin S plaque staining and analyzed using semi-quantitative method (Scale bars, 50μm and 20μm, respectively) (C, D). APP and

BACE1 protein and gene expressions in mice hippocampal tissue were detected by western blotting and qRT-PCR, and then analyzed semi-quantitatively (E-I). Data represent mean ± SD from multi-group experiments. *p < 0.05, **p < 0.01, and ***p < 0.001 (n = 3 each group).

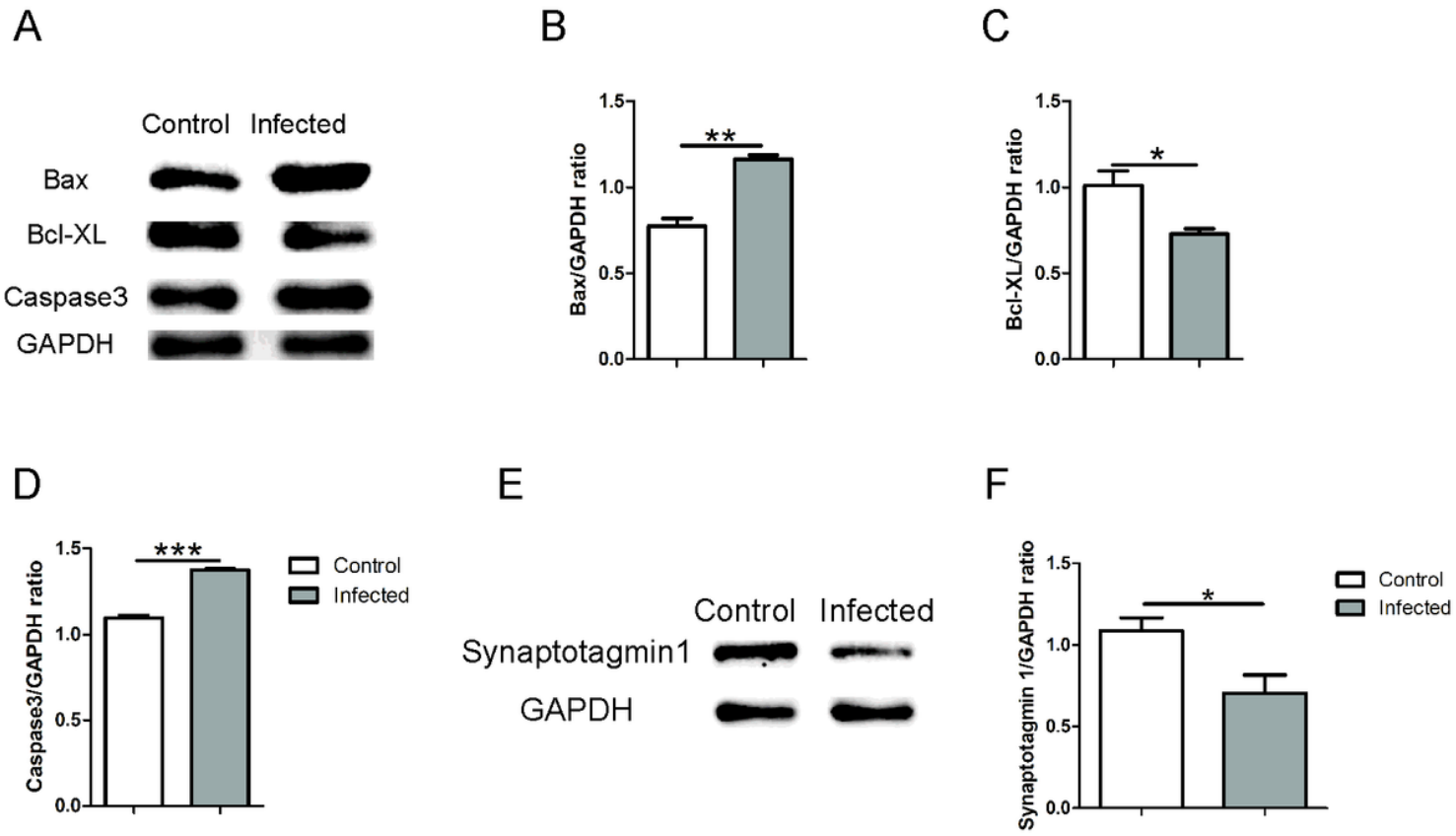

Figure 4

TgCtwh6 infection affected apoptosis-related and synaptotagmin1 proteins expression in HT22. The expression of apoptosis-related proteins in HT22 cells were measured by western blotting (A-D). Besides, synaptotagmin1 protein was detected by western blotting, too (E-F). Data represent mean ± SD from multi-group experiments. *p < 0.05, **p < 0.01, and ***p < 0.001 (n = 3 each group).

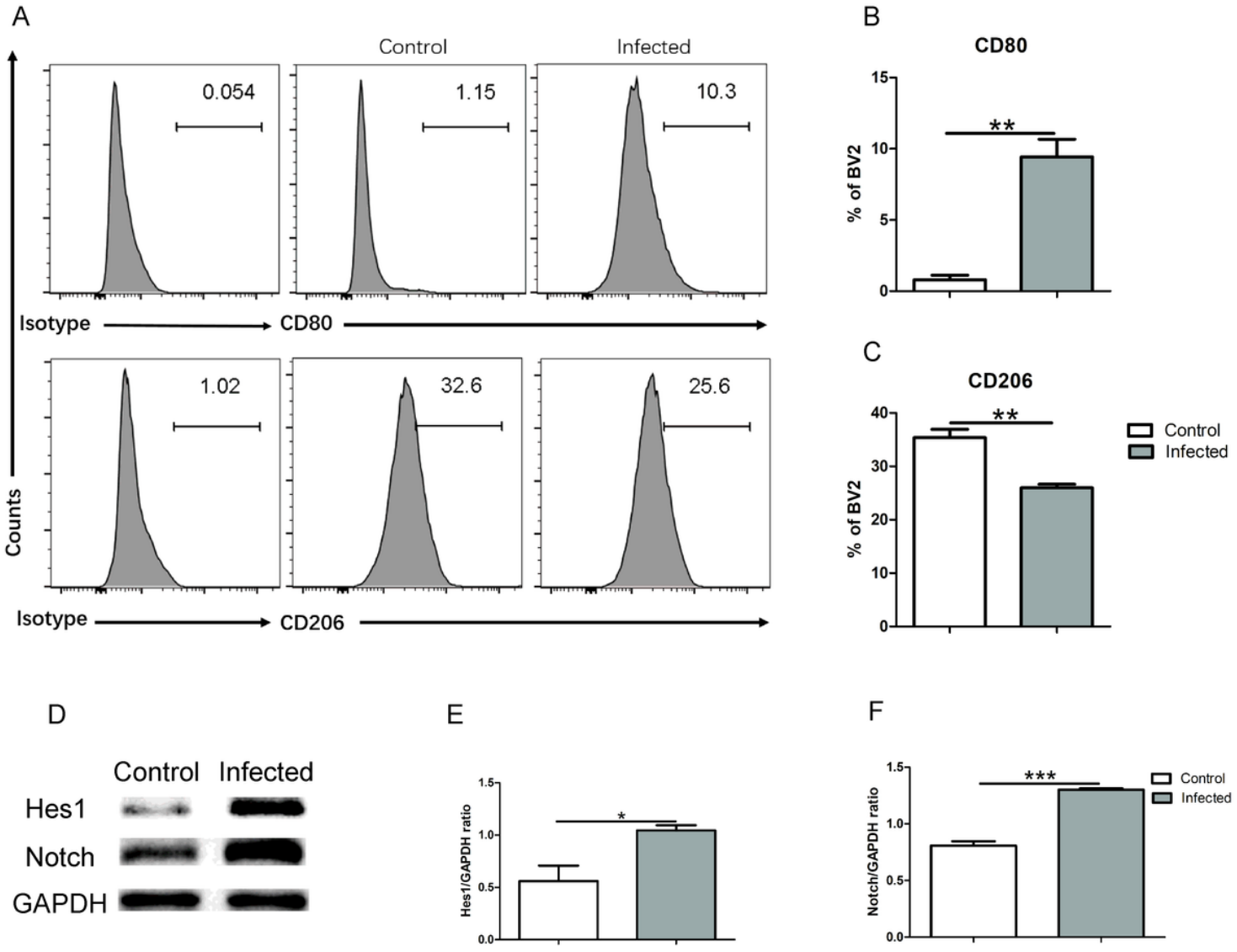

Figure 5

TgCtwh6 infection polarized BV2 into M1 perhaps via Notch signaling. After BV2 were co-cultured with TgCtwh6 for 24 h, BV2 were collected and assessed quantitatively for polarization status using FCM (A-C). Additionally, Notch and Hes1 proteins were detected by western blotting and analyzed by semi-quantitative method (D-F). Data represent mean ± SD from multi-group experiments. *p < 0.05, **p < 0.01, and ***p < 0.001 (n = 3 each group).

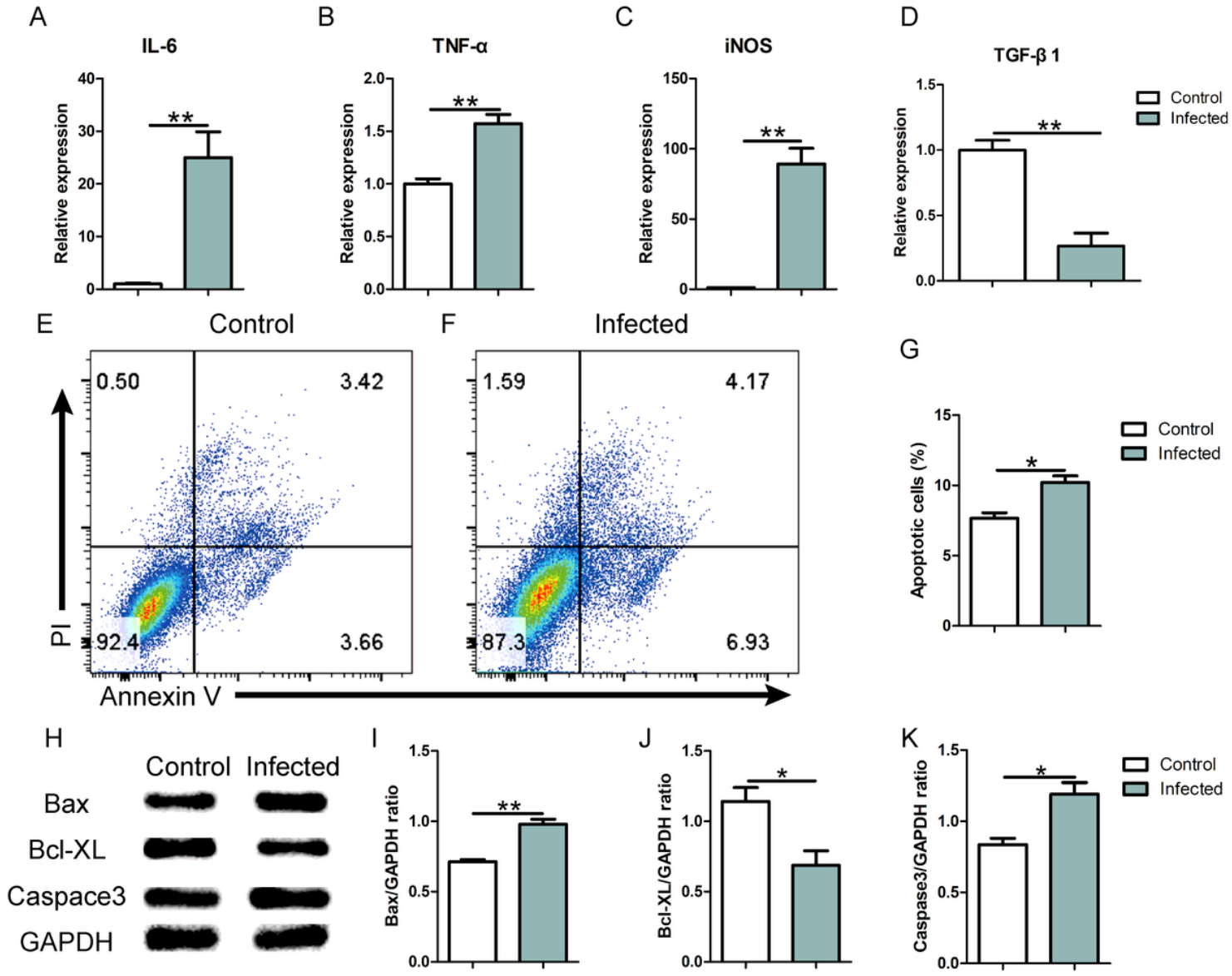

Figure 6

TgCtwh6 indirectly induced HT22 apoptosis by activating BV2 into M1. RNA was extracted from BV2 infected with TgCtwh6 and the gene expression of IL-6, TNF-α, iNOS and TGF-β1 were analyzed by qRT-PCR (A-D). HT22 were collected from the co-cultured system and the apoptosis was assayed by FCM (E-G). HT22 were collected from the co-cultured system and the protein expressions of Bax, Bcl-XL and Caspase3 were detected using western blotting (H-K). Data represent mean ± SD from multi-group experiments.*p < 0.05, **p < 0.01, and ***p < 0.001 (n = 3 each group).

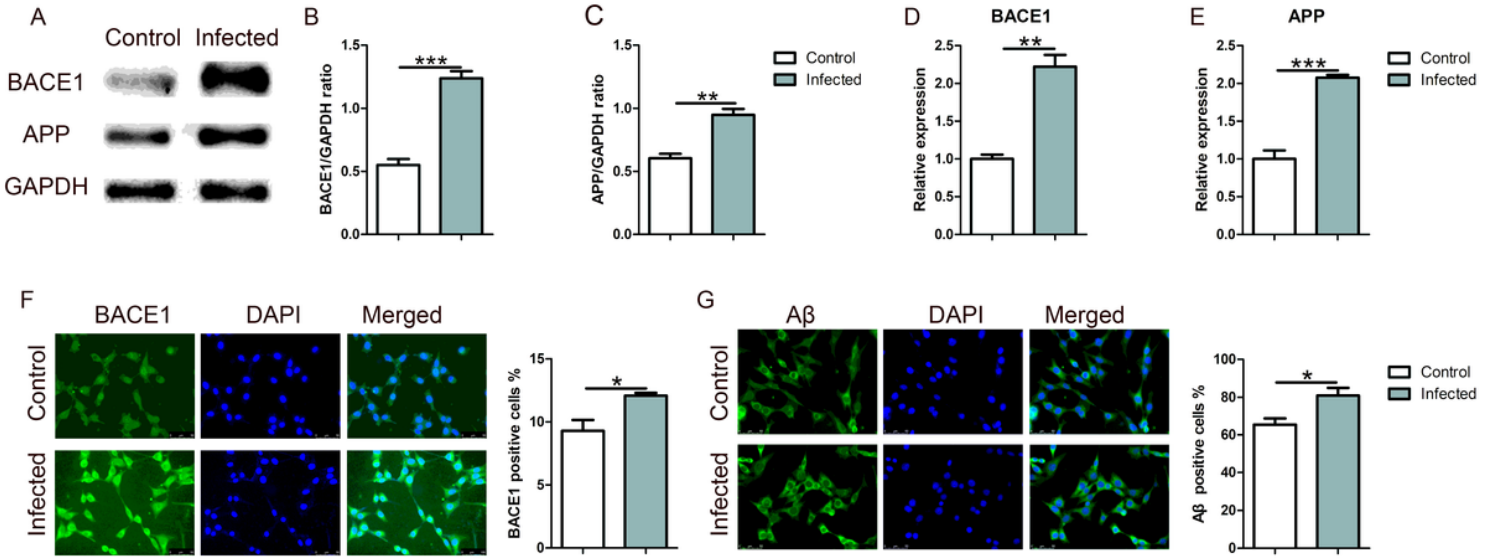

Figure 7

TgCtwh6 infection resulted in APP, BACE1 and Aβ expression in HT22. The protein and gene expression of APP and BACE1 in infected HT22 were determined by western blotting and qRT-PCR, respectively, and then analyzed semi-quantitatively (A-E). The BACE1 and Aβ protein expression in infected HT22 were assayed by immunofluorescence staining and analyzed by semi-quantitative method (F-G). Data represent mean ± SD from multi-group experiments. *p < 0.05, **p < 0.01, and ***p < 0.001 (n = 3 each group).

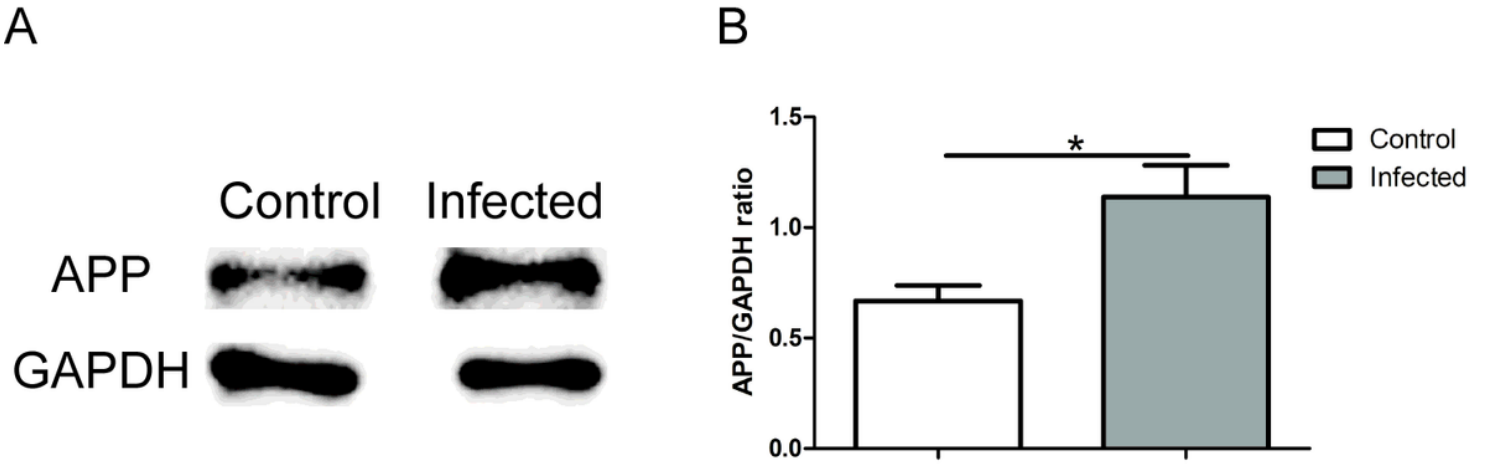

Figure 8

TgCtwh6 indirectly induced BACE1, APP and Aβ secretion from HT22 by activating BV2 into M1. BV2 cells infected with TgCtwh6 were co-cultured with HT22 cells. Then western blotting was used to detect the protein expression of APP in HT22 (A, B). Data represent mean ± SD from multi-group experiments.*p < 0.05, **p < 0.01, and ***p < 0.001 (n = 3 each group).

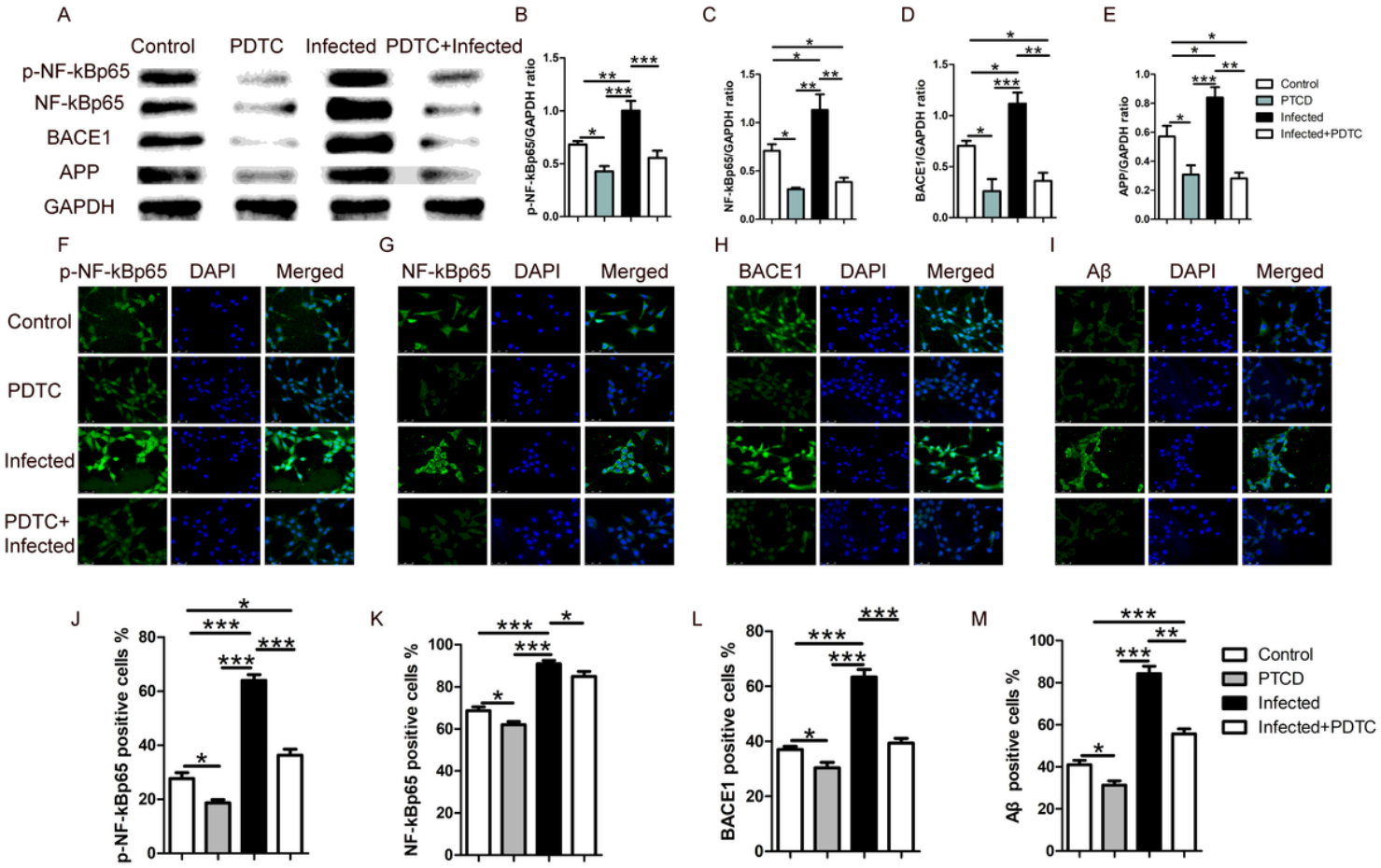

Figure 9

TgCtwh6 infection induced Aβ production by activating NF-κB signaling in HT22. NF-κBp65, p-NF-κBp65, BACE1 and APP in HT22 were evaluated by western blotting and then estimated semi-quantitatively (A-E). Additionally, NF-κBp65, p-NF-κBp65, BACE1 and Aβ proteins in the cytoplasm or nucleus of HT22 were detected using immunofluorescece staining and then analyzed semi-quantitatively (F-M). Data represent mean ± SD from multi-group experiments. *p < 0.05, **p < 0.01, and ***p < 0.001 (n = 3 each group).

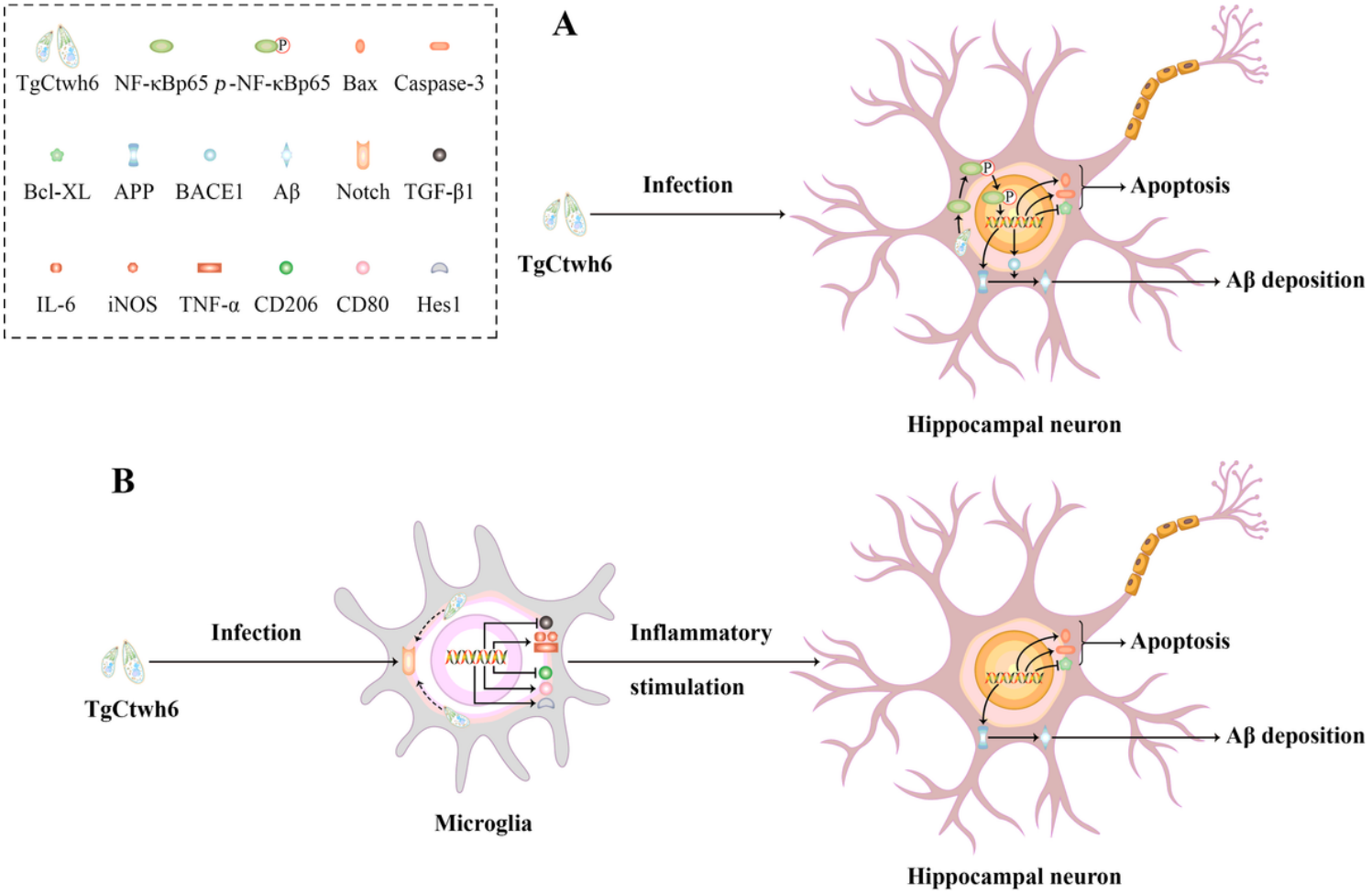

Figure 10

The mechanism with which TgCtwh6 infection induce neuron apoptosis and Aβ deposition in the mouse brain. The direct infection of TgCtwh6 to hippocampal neuron can promote the up-regulation of pro-apoptosis-related proteins Bax, Bcl-XL, and Caspase3 to induce apoptosis of hippocampal neurons. At the same time, TgCtwh6 infection also activates the NF-κB pathway to up-regulate NF-κBp65 and p-NF-κBp65, which increases BACE1, App and Aβ production (A). The infection of TgCtwh6 can activate the Notch signaling in microglia to cause the up-regulation of Hes1 and Notch, which can induce microglia polarization to M1 with the increased expression of CD80 and the decreased expression of CD206. Meanwhile, TgCtwh6 infection stimulates pro-inflammatory factor IL-6, TNF-α, iNOS, but inhibits anti-inflammatory factor TGF-β1 secretions from microglial, leading to the increased expression of APP and pro-apoptosis-related proteins Bax, and Caspase3, the declined expression of anti-apoptosis-related protein Bcl-XL. In all, TgCtwh6 infection can indirectly lead to hippocampal neuronal apoptosis and Aβ deposition through inducing microglial polarization (B).